LAWRENCE
LIVERMORE
NATIONAL
LABORATORY

LLNL-TR-686862

A New Approach to Charged Particle Slowing Down and Dispersion

D. E. Stevens

March 24, 2016

Disclaimer

This work performed under the auspices of the U.S. Department of Energy by Lawrence Livermore National Laboratory under Contract DE-AC52-07NA27344.

A New Approach to Charged Particle Slowing Down and Dispersion *

David Stevens †

March 22, 2016

1 Introduction

The process by which super-thermal ions slow down against background Coulomb potentials arises in many fields of study. In particular, this is one of the main mechanisms by which the mass and energy from the reaction products of fusion reactions is deposited back into the background. Many of these fields are characterized by length and time scales that are the same magnitude as the range and duration of the trajectory of these particles, before they thermalize into the background. This requires numerical simulation of this slowing down process through numerically integrating the velocities and energies of these particles.

The slowing down process can be reduced to considering the properties of an initially uni-directional pulse of super-thermal ions, whose velocity is much greater than the average background ion thermal velocity, $v_p \gg v_{i,th}$. The Coulomb interactons between the pulse and the background plasma cause the pulse of ions to slow down and disperse via deflection and straggling. The rate at which Coulomb interactions decreases the energy of the particle beam is called the charged particle stopping power, $\frac{DE_p}{Dt}$, due to its units of erg/s. The rate at which the beam disperses laterally is called deflection and dispersion along the original direction of the beam is referred to as straggling.

This paper first presents a simple introduction to the required plasma physics, followed by the description of the numerical integration used to integrate a beam of particles. This algorithm is unique in that it combines in an integrated manner both a second-order integration of the slowing down with the particle beam dispersion. These two processes are typically computed in isolation from each other. A simple test problem of a beam of alpha particles slowing down against an inert background of deuterium and tritium with varying properties of both the beam and the background illustrate the utility of the algorithm. This is followed by conclusions and appendices. The appendices define the notation, units, and several useful identities.

2 Slowing Down Derivation

An excellent starting place for this derivation is the simple discussion of the deflection caused by the Coulomb interactions between two charged particles presented in the monograph by Spizter[1]. This simple Rutherford scattering is described by the the formula for the deflection of the two particles given by

$$\tan\theta/2 = \frac{Z_1 Z_2 e^2}{M p v^2} \tag{1}$$

where M is the reduced mass, $M = 1/m_1 + 1/m_2$, v is the relative velocity of the particles, p is the impact parameter which represents the distance of closest approach given no Coulomb forces, and θ is the angular deflection of each particle. The

*This work was performed under the auspices of the U.S. Department of Energy by the University of California, Lawrence Livermore National Laboratory under contract No. W-7405-Eng-48

†Lawrence Livermore National Laboratory

momentum and energy deposition that results is found by integrating over all of the particles that interact. Unfortunately, this simple integration yields an unbounded integral if the maximum impact parameter is not limited in some fashion.

An excellent discussion of this deposition is provided in Chapter 11 of Atzeni and Meyer-Ter-Vehn (hereafter AM)[2] for the stopping of an ion against the electrons in a plasma, which is repeated below and is similar in spirit to the discussion in the Spitzer monograph. The momentum and energy exchange between an electron and an ion in a Coulomb collision is given by:

$$\Delta p^2 = \frac{(2m_e v_p)^2}{1+(b/r_o)^2} \tag{2}$$

$$\Delta E_p = \left(\frac{2Z^{*2}e^4}{m_e v_p^2}\right)\frac{1}{b^2+r_o^2} \tag{3}$$

$$r_o = \frac{Z^* e^2}{m_e v_p^2} \tag{4}$$

assuming an effective ionization of Z^* for the ion. The net change in the ion's energy dE as it traverses a segment dx for an impact parameter b is given by the number of electron interactions in the circle of circumference $2\pi b$ and given by the expression: $2\pi b n_e db$. This yields the integral

$$\frac{DE}{Dx}|_e = \frac{4\pi Z^2 e^4 n_e}{m_e v_p^2}\int_0^{b_{max}}\frac{bdb}{b^2+r_o^2} \tag{5}$$

$$= \frac{4\pi Z^2 e^4 n_e}{m_e v_p^2}\left(\frac{1}{2}\log(1+\frac{b_{max}^2}{r_o^2})\right) \tag{6}$$

$$= \frac{4\pi Z^2 e^4 n_e}{m_e v_p^2}\log\Lambda_e \tag{7}$$

where b_{max} is chosen to eliminate the divergence of the integral from the true maximum limit of infinity. This limit has the physical justification that the interaction of far-field ions cancels out or screens the effect of far-field electrons allowing this integral to be truncated. The most commonly used limit is the Debye length, defined by $\lambda_D^2 = kT_e/(4\pi n_e e^2)$. There are limits to the direct usage of above result, such as for cases where the minimum impact parameter is better obtained from quantum mechanical considerations instead of the Landau length, r_o. The above derivation is useful though as it determines the functional form of the ion slowing down and introduces the concept of the Coulomb logarithm, $\log\Lambda_e$.

There are several alternate derivations of the stopping power of ions against both electrons and ions. These typically take into account the fact that as the ion traverses the plasma, it has a many body wake effect that needs to be considered in more accurate approximations. One such approach is given by Brown Preston and Singleton (BPS) [3] that avoids the introduction of a Coulomb logarithm altogether.

The above derivation for simplicity used the fact that the mass of an electron is much less than a typical super-thermal ion to ignore center of mass considerations. In general, one must take into account the motion of the center of mass of the colliding particle with the background Maxwellian distribution of field particles, electrons and ions. The Coulomb interactions also lead to dispersion of the beam by deflection and straggling. These center of mass considerations yield the following rate equations for the beam slowing down, deflection, and straggling respectively. These expressions were initially derived by Chandrasekhar in the context of stellar evolution [4].

$$\frac{\partial v_{p,f}}{\partial t} = -A(1+\frac{m_p}{m_f})\frac{G(y_f)}{v_{f,th}^2} \tag{8}$$

$$\frac{\partial < v_{p,f,\perp} >^2}{\partial t} = A\frac{\mathrm{erf}(y_f)-G(y_f)}{v_p} \tag{9}$$

$$\frac{\partial < v_{p,f,\parallel} >^2}{\partial t} = A\frac{G(y_f)}{v_p} \tag{10}$$

where the function G is given by

$$G(y_f) = \frac{\mathrm{erf}(y_f) - \frac{2}{\sqrt{\pi}} y_f \exp(-y_f^2)}{2y_f^2} \tag{11}$$

and A by:

$$A = \frac{8\pi Z^2 Z_f^2 e^4 n_f}{m_p m_{p,f}} \log \Lambda_{p,f} \tag{12}$$

where $m_{p,f} = m_p m_f/(m_p + m_f)$ is the reduced mass, $y_{p,f} = v_p/v_{f,th}$ is a scaled velocity and $v_{f,th}^2 = 2kT_f/m_f$ is the thermal velocity of field particle, f. These three equations form a foundation for any theoretical treatment of charged particles interacting with a plasma. The total slowing down of the charged particle is found by the sum over all the field particles f that make up the background, b, and is given by:

$$\frac{DE_p}{Dt} = m_p v_p \sum_{f \in b} \frac{\partial v_{p,f}}{\partial t} \Rightarrow \frac{DE_p}{Dx} = m_p \sum_{f \in b} \frac{\partial v_{p,f}}{\partial t} \tag{13}$$

This results in the following sum which is equivalent to the Equations 11.85 through 11.87 of AM in slightly modified form:

$$\frac{Dv_p}{Dt} = \frac{4\pi Z_p^2 e^4}{m_p v_p^2} \sum_{f \in b} \frac{n_f Z_f^2}{m_{pf}} \log \Lambda_{pf} \hat{G}(y_{pf}) \tag{14}$$

$$\frac{DE_p}{Dx} = \frac{4\pi Z_p^2 e^4}{v_p^2} \sum_{f \in b} \frac{n_f Z_f^2}{m_{pf}} \log \Lambda_{pf} \hat{G}(Y_{pf}) \tag{15}$$

where $\hat{G}(y) = \mathrm{erf}(y) - \frac{2}{\sqrt{\pi}} y_f \exp(-y_f^2)$

2.1 Coulomb Logarithms

The variety of Coulomb logarithms that could be explored is quite large. The focus of this document on the numerical algorithm for integrating a particle beam allows the use of simple ion and electron Coulomb logarithms. The Coulomb logarithms used here follow:

$$f(y) = \frac{0.321 + 0.259y + 0.0707y^2 + 0.05y^3}{1 + 0.130y + 0.0500y^2} \tag{16}$$

$$\omega^2 = \frac{4.0\pi e^2 n_e}{m_e} \tag{17}$$

$$\Lambda_e = \frac{2m_e v_{e,th}}{\hbar\omega} f(y_e^2) \tag{18}$$

$$\log \Lambda_e = 0.5 \log(1 + \Lambda_e^2) \tag{19}$$

$$b_{max} = \lambda_D \tag{20}$$

$$\Lambda_i^2 = \frac{(2.377 \times 10^{23}) T_e^2 b_{max}^2}{15.961 + T_e} \tag{21}$$

$$\log \Lambda_i = \log(\Lambda_i) \tag{22}$$

The function $f(y)$ is a function that fits the electron Coulomb logarithm to the stopping power analysis in Maynard and Deutsch [5]. This choice of Coulomb logs is more fully described in Zimmerman [6].

2.2 Electron Thermal Velocity

Practical use of the following algorithm requires at least a simple treatment of electron degeneracy. The thermal velocity of electrons in a degenerate plasma needs to be corrected from the ideal, $v_{e,th}^2 = 2k_b T_e/m_e$. Electron degeneracy is taken into account

here by a degeneracy parameter: ζ via

$$e_F = \frac{\hbar^2}{2m_e}(3\pi^2 n_e)^{2/3} = k_b T_f \tag{23}$$

$$x = \sqrt{\frac{e_F}{K_b T_e}} \tag{24}$$

$$\zeta = \frac{(\zeta_0 + x(0.1679 + x(0.3108)))x^3}{1 + x(0.2676 + x(0.2280 + x(0.3099)))} \tag{25}$$

The corrected thermal electron velocity is calculated by the expression:

$$v_{e,th} = \frac{\hbar\sqrt{\pi}}{m_e}\left(\frac{4n_e}{1.0 - \exp(-\zeta)}\right)^{1/3} \tag{26}$$

3 Numerical Integration

This approach for integrating an ensemble of charged particles as discrete Monte Carlo particles consists of two parts. The first part consists of a second-order integration of the range of the simulated charged particle over a timestep that accounts for the slowing down, followed by adding a random velocity correction at the end of the timestep that accounts for the deflection and straggling using particle information from the start of the timestep to compute the Gaussian distribution of dispersion. This numerical treatment is a simple Stochastic Differential Equation (SDE) integration of the Euler-Maruyama variety with well known strong and weak convergence properties [7]. There are extensions of this technique to higher order methods for SDE integration, such as the Milstein method [8], which is a subject for future work.

The slowing down and range calculation starts from Equation 14, where after some manipulation:

$$\frac{Dv_p}{Dt} = v_p \frac{Dv_p}{Dx} \tag{27}$$

$$\frac{Dv_p}{Dx} = \frac{1}{\tau_e}\left(\frac{1}{2z^3} + \frac{1}{2\phi(y)}\right) \tag{28}$$

These equations are supported by the following definitions

$$\eta = \frac{4}{3\sqrt{\pi}}\left(\frac{n_e/m_e \log\Lambda_e}{n_i Z_{eff}^2/m_i \log\Lambda_i}\right) \tag{29}$$

$$v_c = \frac{v_{e,th}}{\eta^{1/3}} \tag{30}$$

$$y = v_p/v_{e,th} \tag{31}$$

$$z = v_p/v_c \tag{32}$$

The function ϕ is given by:

$$\phi(y) = \frac{4}{3\sqrt{\pi}}\frac{y^3}{\hat{G}(y)} \tag{33}$$

and approximated numerically by:

$$\phi(y) = 1 + \frac{((((0.09744y - 0.05352)y + 0.18797)y + 0.00517)y + 0.6)y^2}{1 + ((0.12953y - 0.05468)y + 0.02978)y} \tag{34}$$

The timescale τ_e provides the dimensional time scale of the process and is given by its reciprocal:

$$\frac{1}{\tau_e} = \left(\frac{n_e}{m_e}\log\Lambda_e\right)\frac{32\sqrt{\pi}}{3v_{e,th}}\frac{e^4 Z_p^2}{m_p} \tag{35}$$

This equation is integrated in the following section.

The second step of deflection and straggling integration follows the approach of Sherlock [9] which samples the dispersion distribution via two Gaussian random numbers, $N(\sigma_{\parallel})$ and $N(\sigma_{\perp})$, where the variance of these random numbers is given by

$$\begin{aligned} \sigma_{\parallel} &= \sqrt{\Delta t \frac{\partial < v_{p,f,\parallel} >^2}{\partial t}} \\ \sigma_{\perp} &= \sqrt{\Delta t \frac{\partial < v_{p,f,\perp} >^2}{\partial t}} \end{aligned} \tag{36}$$

These two random numbers represent a normal and a tangential perturbation velocity that are then applied to the final velocity of the range calculation.

3.1 The Slowing down and range numerical integration

The slowing down integration is a second-order approach, in the non dimensional z velocity, which integrates the charged particle velocity from z_{init} to z_{final} along a single segment of the particles trajectory. This approach follows that of an earlier effort by Zimmerman [10] due to its robustness and ease of implementation. The trajectory of the particle is the sum of all the segments needed for the particle to thermalize into the background. This approach is complicated by the need to observe stable limits for the timestep of each segment, Δt and its length, l. This algorithm simplifies this concern by the use of an elegant estimate of the timestep

$$\Delta t = \frac{2l}{z_{init} + z_{final}} \tag{37}$$

and the identities

$$z^2 = z_{init}^2 + \frac{2l}{v_c^2}\frac{Dv_p}{Dt} \tag{38}$$

$$z = z_{init}^2 + \frac{\Delta T}{v_c}\frac{Dv_p}{Dt} \tag{39}$$

These two identities allow one to convert any limitation on distance traveled or timestep into a velocity limitation. These limitations can also arise from the need to prevent the particles crossing region boundaries or the need to synchronize the simulation on a census time. Thus, all the limitations on the size of a segment can be converted into an estimate of the final velocity. The limitation that controls the length of the segment is the the one that results in the minimum allowable changes in velocity. This algorithm uses a two step Runge-Kutta process that starts with an initial defined minimum allowable distance l_{min} and timestep Δt_{min}.

1. Estimate the final energy and velocity via the forward Euler step

$$z_1^2 = z_{init}^2 + \frac{2l_{min}}{v_c^2}\frac{Dv_p}{Dt} \tag{40}$$

$$z_2^2 = z_{init}^2 + \frac{\Delta T_{min}}{v_c}\frac{Dv_p}{Dt} \tag{41}$$

$$\tag{42}$$

2. Compute the midpoint velocity of the step via the midpoint rule

$$z_{mid} = \frac{1}{2}\left(z_{init} + \max(z_1, z_2, z_{other})\right) \tag{43}$$

where z_{other} can be any other limiting velocity for the segment such as estimates of the rate of change of the underlying Coulomb logarithms.

3. Calculate $\frac{Dv_p}{Dt}_{mid}$ using the midpoint velocity, z_{mid} from Equation 27.

4. repeat step 1 using the more accurate velocity derivative.

5. The velocity of the segment taking into account only slowing down is given by $z_{sd} = \max(z_1, z_2, z_{other})$ which allows the range and duration of the segment to be calculated via:

$$l = \frac{z_{sd}^2 - z_{init}^2}{2v_c \frac{Dv_p}{Dt}_{mid}} \tag{44}$$

$$\Delta t = v_c(z_{init} - z_{sd}) \frac{Dv_p}{Dt}_{mid} \tag{45}$$

3.2 Dispersion

The correction of the charged particle velocity for dispersion first computes the variance of the dispersion via Equation 36 and samples the resulting Gaussian random numbers, $N(\sigma_\parallel)$ and $N(\sigma_\perp)$. These are used as velocity perturbations in both the normal and tangential directions, which are applied as follows. Given the initial direction cosine vector, (n_x, n_y, n_z) of the particle, two orthogonal tangential coordinate directions are computed via:

$$\alpha = \sqrt{2(1 - n_x n_y - n_x n_z - n_y n_z)} \tag{46}$$

$$\begin{bmatrix} t_x \\ t_y \\ t_z \end{bmatrix} = \frac{1}{\alpha} \begin{bmatrix} n_y - n_z \\ n_z - n_x \\ n_x - n_y \end{bmatrix} \tag{47}$$

$$\begin{bmatrix} w_x \\ w_y \\ w_z \end{bmatrix} = \frac{1}{\alpha} \begin{bmatrix} n_x(n_y + n_z) - n_y n_y - n_z n_z \\ n_y(n_x + n_z) - n_x n_x - n_z n_z \\ n_z(n_x + n_y) - n_x n_x - n_y n_y \end{bmatrix} \tag{48}$$

This estimate of the tangential directions is ill-defined if $|n_x - n_y| < \varepsilon$ and $|n_z - n_y| < \varepsilon$, where ε is the floating point tolerance of the simulation. In this case:

$$\alpha = \sqrt{2(1 + n_z(n_y - n_x) + n_x n_y)} \tag{49}$$

$$\begin{bmatrix} t_x \\ t_y \\ t_z \end{bmatrix} = \frac{1}{\alpha} \begin{bmatrix} n_y + n_z \\ n_z - n_x \\ -n_x - n_y \end{bmatrix} \tag{50}$$

$$\begin{bmatrix} w_x \\ w_y \\ w_z \end{bmatrix} = \frac{1}{\alpha} \begin{bmatrix} n_x(n_z - n_y) - n_y n_y - n_z n_z \\ n_y(n_x + n_z) - n_x n_x - n_z n_z \\ n_z(n_x - n_y) - n_x n_x - n_y n_y \end{bmatrix} \tag{51}$$

The velocity perturbation due to deflection and straggling can now be computed via a uniformly distributed random number, ξ such that $-\pi < \xi < \pi$, and the vector:

$$\begin{bmatrix} dv_n \\ dv_t \\ dv_w \end{bmatrix} = \begin{bmatrix} N(\sigma_\parallel) \\ N(\sigma_\perp)\cos(\xi) \\ N(\sigma_\perp)\sin(\xi) \end{bmatrix} \tag{52}$$

The final velocity of the particle can now be computed via matrix multiplication

$$\begin{bmatrix} v_{p,x}^{final} \\ v_{p,y}^{final} \\ v_{p,z}^{final} \end{bmatrix} = \begin{bmatrix} v_{p,x}^{sd} \\ v_{p,y}^{sd} \\ v_{p,z}^{sd} \end{bmatrix} + \begin{bmatrix} n_x & t_x & w_x \\ n_y & t_y & w_y \\ n_z & t_z & w_z \end{bmatrix} \begin{bmatrix} dv_n \\ dv_t \\ dv_w \end{bmatrix} \tag{53}$$

where v_p^{sd} is the particle velocity after the slowing down has been computed and the particle moved along its segment.

The energy deposition from the combined algorithm is a two step process. Once the slowing down component of the segment is computed, the energy of the particle E_{sd} before disperision is known. This allows the energy deposition to be initialized via:

$$\begin{aligned} \Delta E_{sd} &= E_0 - E_{sd} && (54) \\ \Delta E_i &= f_{mid}\Delta E_{sd} && (55) \\ \Delta E_e &= (1-f_{mid})\Delta E_{sd} && (56) \end{aligned}$$

where the quantity $f_{mid} = 1/(1+z_{mid}^3/\phi(y_{mid}))$ is the local electron-ion split of the energy deposition on the segment that arises from Equation 28. Statistically the deflection and straggling algorithm has a mean of zero and should conserve energy analytically requiring no explicit energy deposition. However, it was found that it was necessary to conserve energy exactly, by removing energy from the background if the particle was accelerated by the dispersion or adding energy if the particle was decelerated, which should also statistically have a mean of zero deposition. This is accomplished by modifying the energy deposition via the correction:

$$\begin{aligned} \Delta E_i &= \Delta E_i - g_{mid}(E_{final} - E_{sd}) && (57) \\ \Delta E_e &= \Delta E_e - (1-g_{mid})(E_{final} - E_{sd}) && (58) \end{aligned}$$

where $g_{mid} = f_{mid}$ if both electron and ion deflection and straggling are computed. If only deflection and straggling due to the ions is included, $g_{mid} = 1$.

3.3 Thermalization

The numerical integration is complete when the tracked charged particle has lost sufficient energy to be merged back into the background. The stopping criterion for this process is when the particle at the end of the slowing down step has energy less than $3/2kT_i$. Then, the particle residual mass and energy is deposited to the background.

4 Results

The evaluation of this algorithm was performed on an initially uni-directional in x beam of alpha particle in a non-reacting DT equimolar plasma. The reference conditions were motivated by the problem by Johzaki [11] where the background was at a density of 20 g/cc and temperature of 5 keV. The beam is initially 10^{10} 3.5 MeV energy alpha particles and is emitted over a 50 picosecond span, although the duration of the source is not constraining as the particles are non-reacting in this test problem and cannot create any knock on upscattering or cause any reaction in flight (RIF) reactions. 10^6 Monte Carlo particles were used to model this beam of particles and were emitted at $x = 120$ microns in a $480 \times 120 \times 120$ micron domain, where the long dimension is in the x direction.

The behavior of the slowing down and dispersion algorithms were analyzed by the following scans keeping the background isothermal with $T_e = T_i$.

Fix $\rho = 20$g/cc, $E_p = 3.5$MeV	Vary T_e: 1, 2, 5, 10, 20, 50, 100, 150, 200 keV.
Fix $T_e = 10$keV, $E_p = 3.5$MeV	Vary ρ: 3.5, 5.0, 7.5, 10, 12.5, 15.0, 20.0, 25.0, 30.0 g/cc.
Fix $\rho = 20$g/cc, $T_e = 10$keV	Vary E_p: 0.1, 0.2, 0.5, 1.0, 2.0, 3.5, 5.0, 10.0, 15.5 MeV.

Each of these scans probes different dependencies of the dispersion and slowing down algorithms. The temperature scan controls the scaling of the y parameter. The particle energy scan probes additional dependencies on the particle velocity, and the density scan probes primarily the dependence on n_e and n_i.

Figure 1 shows the temporal energy deposition for the 10 g/cc and 5 keV initial conditions. The temporal dependence of the beam shows that initially most of the energy in the beam is depositing against the electron background with the deposition to the

ion field becoming more prominent as the beam loses sufficient energy and thermalizes. Figure 2 shows the spatial energy and mass deposition profiles that have been integrated over time. The effect of straggling is clearly present as seen by the Gaussian shape of the mass deposition and the leading edge of the energy deposition to the background ions.

The role of straggling and deflection on mass deposition is also shown in Figure 3 which averages all of the deposition in the z direction in each pixel which extends out of the page. The Monte Carlo nature of the simulation is observed for the 50 keV case with some minor statistical fluctuation being observed due to lack of statistics for only 10^6 simulation particles.

The comparison of variations in electron temperature, density, and particle energy are shown in Figures 4-6. The role of increasing temperature on this algorithm is seen by electron energy deposition becoming negligible after $T_e = 50$ keV with the bulk of the energy deposition being due to the ions at that point. Lowering the density of the background for fixed temperature appeased to extend the range of the ion beam and spread out the eventual thermalization. Increasing the initial particle energy appears to have little effect on the total amount of energy deposited to the ions in the background and the width of the eventual dispersion. This is due to the bulk of the energy deposition going to electrons at early time. It appears the particles in this case lose most of their energy to the electrons and only start depositing energy to the ions once their particle energies become roughly equivalent.

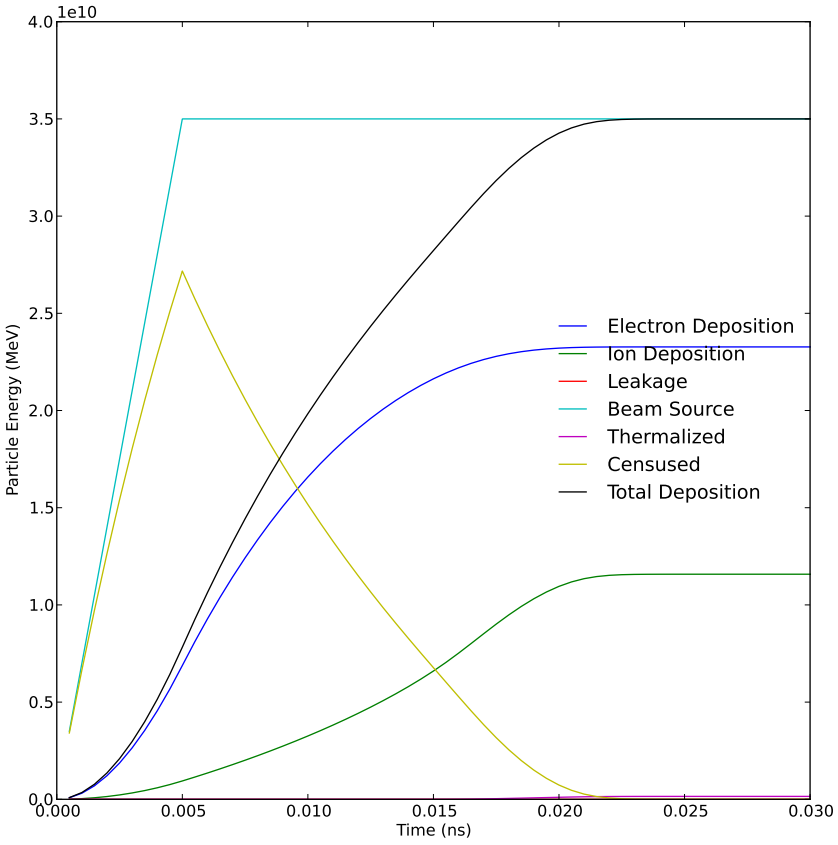

Figure 1: The energy deposition as a function of time for the 10 g/cc and 5 keV background

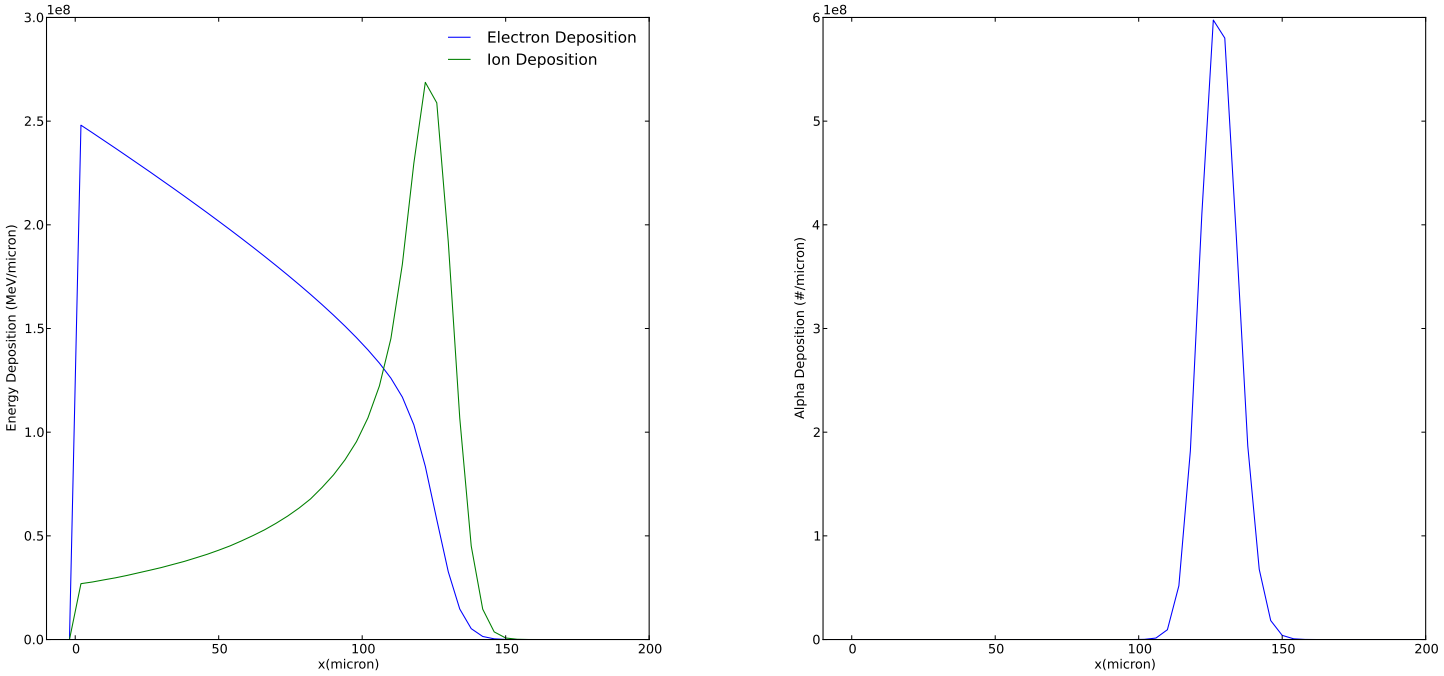

(a) Energy

(b) Mass

Figure 2: The spatial profiles of energy (a) and mass deposition (b) for the 10 g/cc and 5 keV background

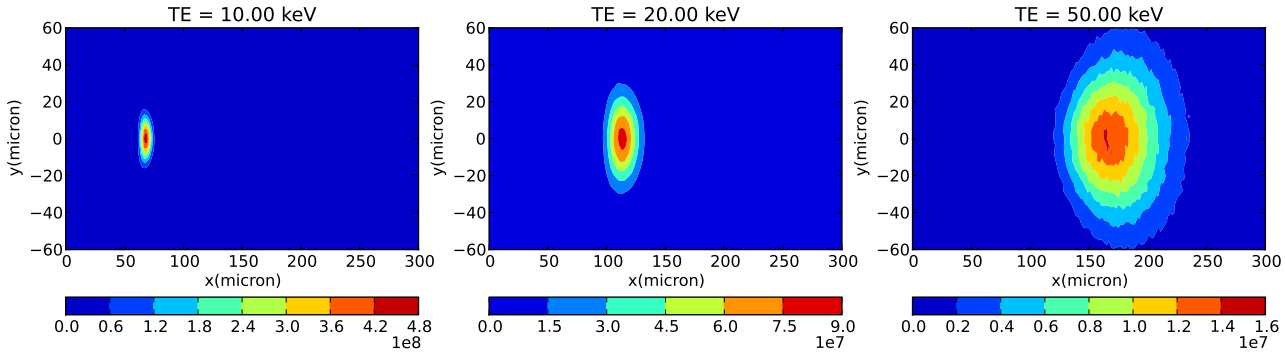

Figure 3: Contour plots of the mass deposition for three temperatures for variations in temperature about the 20 g/cc reference density.

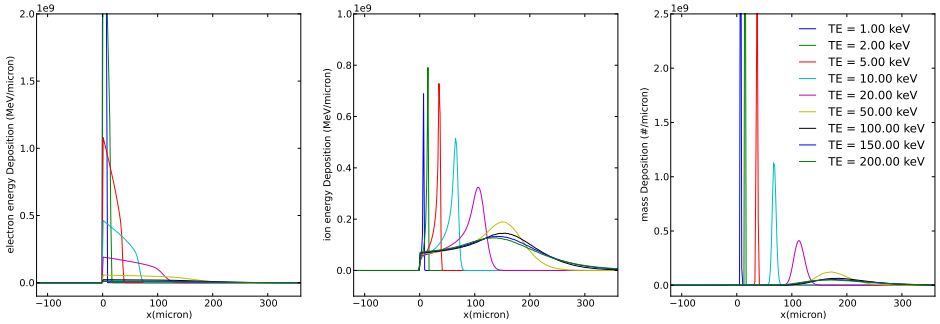

Figure 4: Deposition profiles for the variations in T_e

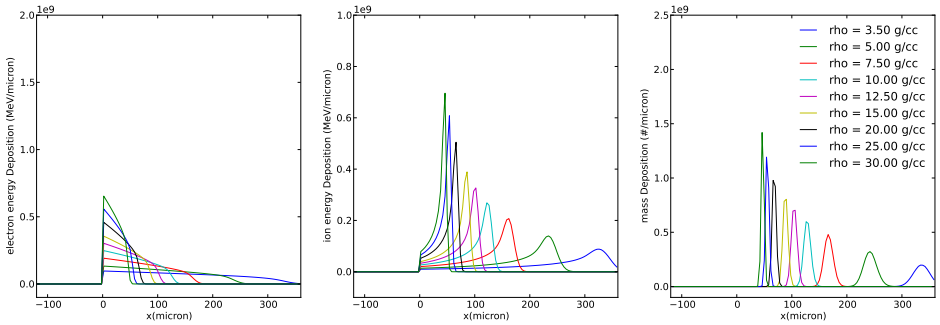

Figure 5: Deposition profiles for the variations in density

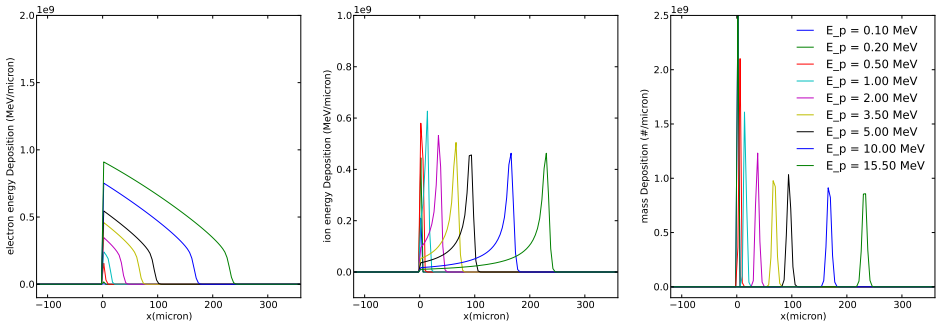

Figure 6: Deposition profiles for the variations in Particle energy

5 Conclusions

This document describes a simple stochastic differential equation (SDE) approach to incorporating both straggling and deflection with a method for integrating charged particle slowing down. The method is promising in that it provides a simple and robust method of obtaining the Gaussian dispersion pattern associated with the Bragg Peak that occurs when charged particles eventually

thermalize back into the background.

A first-order Euler-Murayama approach was used in this algorithm. This appears to be sufficient in capturing the overall behavior desired. However, further improvements in accuracy can be obtained by switching to the more accurate Milstein SDE approach. Dimits [8] provides a method for how the statistics of the dipersion integrals could be incorporated into a Milstein based algorithm. This method is relatively straightforward in implementation requiring a shift from pure Gaussian Random number sampling for the straggling and deflection to tables of pre-computed random number distributions that behave according to the proper double integrals of the noise distribution.

A Basic Definitions

The following definitions of Debye Length, $\lambda_{D,f}$ and plasma frequency, ω_f are used in this document for a background field particle, f:

$$\begin{aligned} v_{f,th}^2 &= 2kT/m_f && (59)\\ &= 2\lambda_{D,f}^2\omega_f^2 && (60)\\ \omega_f^2 &= (4\pi n_f e^2)/m_f && (61)\\ &= v_{f,th}^2/(2\lambda_{D,f}^2) && (62)\\ \lambda_{D,f}^2 &= kT_e/(4\pi n_f e^2) && (63)\\ &= v_{f,th}^2/(2\omega_f^2) && (64) \end{aligned}$$

Note the factor of two in the definition of the electron thermal velocity, $v_{f,th}$!!!. This factor simplifies the specification of the Maxwell Boltzmann distribution below, but complicates comparison with many of the references.

Also, another commonly used expression is the plasma parameter, $\Gamma = Ze^2/(akT)$, which is the ratio of the Coulomb potential of particles with an average interparticle distance, a, to the thermal energy of the background. One interpretation of this is the ability of the thermal ions to overcome this Coulomb potential and potential fuse, thus a criterion for fusion to occur is that $\Gamma \ll 1$.

B Maxwell-Boltzmann Distribution

The Maxwell-Boltzmann distribution is the probability distribution in velocity space that describes a "Maxwellian" background distribution of ions and velocities. This distribution for our choice of thermal velocity, Equation 59 has the convenient form:

$$f(v) = \sqrt{\frac{2}{\pi}}\frac{v^2}{v_{th}^3}\exp\left(-\frac{v^2}{v_{th}^2}\right) \quad (65)$$

The most probable velocity of this distribution is v_{th}, the mean speed is $< v >= 2v_{th}$, and the RMS speed is $< v^2 >= 3v_{th}/2$. These velocity moments are found via the integral over all possible velocities as

$$< v^n >= \int_0^\infty v^n f(v) dv \quad (66)$$

C Units

The units used in this document are an augmented form of the Gaussian system of units where the units of length, time, and mass are, g, cm, and s. This system was chosen over the CGS system, since the electron charge appear primarily in its squared

form $e^2 = 2.307 \times 10^{19}$ erg-cm. This avoids the need to explicitly include the dielectric constant, ε_0, in any of the equations. We augment this system by representing super-thermal particle energies in MeV and temperatures of the background plasma in keV as this keeps the quantities of interest of unit order. This requires the use of the Boltzmann Constant $k = 1.602 \times 10^{-12}$ erg/eV in many of the following equations.

Converting back and forth from the Gaussian units is done via Coulomb's Law:

$$F_c = \frac{1}{4\pi\varepsilon_o}\frac{q_1 q_2}{r^2} = \frac{Z_1 Z_2 e^2}{r^2} \tag{67}$$

where q_1 is the charge of a particle in C, Z_1 is the ionization of a particle, and r is the separation of the two particles.

D Constants

The constants used follow along with some helpful unit conversion into the Gaussian unit system

$\pi = 3.141592653589793$	π
$e = 2.718281828459045$	e
$N_a = 6.022140857^{23}\text{mole}^{-1}$	Avogadro Constant or particles in a mole
$e^2 = 2.307077107 \times 10^{-19}$ erg-cm	electron charge squared
$e = 4.803204401 \times 10^{-10}\sqrt{\text{erg-cm}}$	electron charge
$\varepsilon_o = 8.854187817620 \times 10^{-12}$ F/M	SI vacuum dielectric constant $F = C^2 N^{-1} M^{-2}$
$h = 6.626070040 \times 10^{-27}$ erg s	Planck's Constant
$\hbar = h/(2\pi) = 1.054571800 \times 10^{-27}$ erg s	scaled Planck's Constant
$c = 2.99792458 \times 10^{10}$ cm/s	speed of light in a vacuum
$e_{charge} = 1.6021766208 \times 10^{-19}$ C	electron charge in Coulombs
$m_n = 1.67492728 \times 10^{-24}$ g	neutron mass
$m_p = 1.67262171 \times 10^{-24}$ g	proton mass
$m_d = 3.34358335 \times 10^{-24}$ g	deuteron mass
$m_a = 6.6446565 \times 10^{-24}$ g	alpha mass
$m_e = 9.1093826 \times 10^{-28}$ g	electron mass
$m_p/m_e = 1836.15267261$	ratio of proton to electron mass
$k = 1.602176565 \times 10^{-12}$ erg/eV	Boltzmann Constant to convert T in eV to erg
$k = 1.602176565 \times 10^{-9}$ erg/keV	to convert T in keV to erg
$k = 8.6173324 \times 10^{5}$ eV/K	to convert T in K to eV
$1\text{ j} = 10^7$ erg	conversion from J to erg

E Notation

The notation used for physical quantities follows

n_p	Number density of transported particles $p \in n, c_i, e, \gamma$
n_e, n_{be}	Number density of free and bound electrons
n_b	Number density of the average background ions
n_i	Number density of superthermal ion species, i
c_i	A superthermal ion species
ρ, P, T	Density, pressure, and Temperature

v, v_j	velocity and velocity in the jth direction
$v_{e,th}, v_{p,th}$	thermal velocities of the background electrons and ions
m_e, m_p, m_n	masses of electrons, protons, ions, and neutrons
e_e, e_i, e_r	Electron, ion and radiation specific energy of the background
T_e, T_i, T_r	Electron, ion and radiation background temperatures
E_e, E_i, E_r	extensive Electron, ion and radiation energies
Z_i, Z_i^*	atom number and ionization of ion species, i
A_i	atomic weight in AMU of ion species, i

The following notation is used to manage mixtures and sums over the background

$$n_{tot} = n_e + n_b \tag{68}$$
$$e_{tot} = e_e + e_i \tag{69}$$
$$\rho = \sum_{i \in b} n_i A_i / N_a \tag{70}$$

The following notation is used for numerical quantities

S	a source term in a continuous PDF
$n, *, n+1$	superscripts used to denote starting, intermediate and final times
$\Delta\psi$	denotes the timestep increment of a quantity ψ

References

[1] L. Spitzer. *Physics of Fully Ionized Gases*. Dover, 1962.

[2] S. Atzeni and J. Meyer-Ter-Vehn. *The Physics of Inertial Fusion*. Oxford Science Publications, 2004.

[3] L. S. Brown, D. L. Preston, and R. L. Singleton Jr. Charged particle motion in a highly ionized plasma. *Physics Reports*, 410(4):237 – 333, 2005.

[4] S. Chandrasekhar. *Principles of Stellar Dynamics*. Dover, 1942.

[5] G. Maynard and C. Deutsch. Born random phase approximation for ion stopping in an arbitrarily degenerate electron fluid. *J. Physique*, 46(7):1113–1122, 1985.

[6] G. B. Zimmerman. Coulomb Physics Models in ICF codes(U). Technical Report LLNL-PRES-422862, LLNL, January 2010.

[7] B. Øcksendal. *Stochastic Differential Equations: An Introduction with Applications*. Springer, 1985.

[8] R.E. Caflisch M.S. Rosin A.M. Dimits, B.I. Cohen and L.F. Ricketson. Higher-order time integration of Coulomb collisions in a plasma using Langevin equations. *JCP*, 242:561–580, 2013.

[9] M. Sherlock. A monte-carlo method for coulomb collisions in hybrid plasma models. *J. Comput. Phys.*, 227:2286–2292, 2008.

[10] G. B. Zimmerman. Charged particle range calculations. private communication, August 2015.

[11] Y. Nakao T. Johzaki, A. Oda and K. Kudo. Accuracy validation of flux limited diffusion models for calculating alpha particle transport in icf plasmas. *Nuclear Fusion*, 39:753.